Pure & Appl. Chem., Vol. 66, No. 6, pp. 1195–1206, 1994.
Printed in Great Britain.
© 1994 IUPAC

Mass and optical emission spectroscopy of plasmas for diamond-synthesis

Carsten Benndorf, Pierre Joeris and Roland Kröger
Department of Physical Chemistry
University of Hamburg, Bundesstrasse 45
D-20146 Hamburg, F.R. Germany

Abstract

From the compilation of literature data Bachmann et al. demonstrated that the diamond synthesis using different deposition techniques (including excitations by microwave, hot-filament, different kinds of arc plasmas as well as flames) occurs in a small area of the ternary C/H/O diagram with two well defined boundaries of binary mole fractions X_C = C/C+O. This "phase diagram" suggests that the plasma chemistry for a defined C/H/O ratio leads to identical radicals and gas phase species, independly from the different source gases.

In order to prove this thesis, we performed a systematic study using different source gases (hydrogen/hydrocarbons/ oxygen) in a microwave deposition system. Informations about the plasma chemistry and its changes due to different gas compositions were gained from mass spectroscopy (MS) and optical emission spectroscopy (OES). The phase purity and the film micro structure of the deposited diamond films were measured using Raman spectroscopy and scanning electron microscopy, respectively.

The influence of oxygen addition was determined for two relevant hydrogen/hydrocarbon (CH_4 and C_2H_2) systems. The possibility to deposit diamond without extra addition of H_2 is demonstrated for $Ar/CH_4/O_2$ and $Ar/C_2H_2/O_2$ plasmas.

1. Introduction

It is well established that different techniques can be applied for the low pressure synthesis of diamond. These techniques include excitations by microwave, hot-filament, different kinds of arc plasmas as well as flames (from acetylene/ oxygen mixtures). The most common gas mixture used in microwave and hot-filament reactors contain a high hydrogen (~99%) and low methane (~1%) content. Atomic hydrogen (from the dissociation in the plasma or hot-filament) is assumed to be an essential ingredient for the removal of unwanted graphitic carbon deposition as well for the production of methyl radicals, consistent with the high H_2 concentrations used in most recent works. Contrary, the diamond deposition from the acetylene flame (using a C_2H_2/O_2 gas mixture with an carbon/oxygen ratio in the range of C/O = 1.02 - 1.18) uses no extra hydrogen in the feed gas.

Recently, Bachmann et al. (1) published a ternary C/H/O "phase diagram" for the low pressure diamond synthesis. From the compilation of literature data they demonstrated that the diamond synthesis occurs in a small area of the ternary C/H/O diagram with two well defined boundaries of binary mole fractions X_C = C/C+O. This "phase diagram" suggests that the plasma chemistry for a defined C/H/O ratio leads to identical radicals and gas phase species, independly from the different source gases.

In order to prove this thesis, we performed a systematic study using different source gases (hydrogen/hydrocarbons/ oxygen) in a microwave diamond deposition system. Informations about the plasma chemistry and its changes due to different gas compositions were obtained from mass spectroscopy (MS) and optical emission spectroscopy (OES); this technique has been applied succesfully by other authors recently (2-5). The phase purity and the film micro structure of the deposited diamond films were measured using Raman spectroscopy and scanning electron microscopy, respectively.

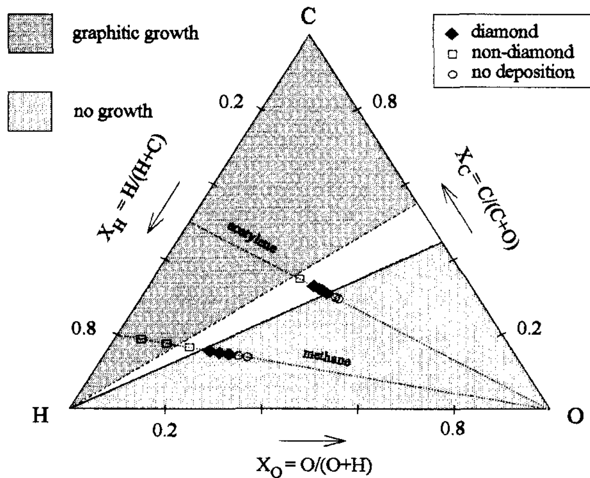

Fig 1. Phase diagram with borders proposed by Bachmann. Shown are the results of our deposition experiments with $Ar/CH_4/O_2$ and $Ar/C_2H_2/O_2$ gas mixtures.

For example, the influence of oxygen addition was measured for two relevant hydrogen/hydrocarbon (CH_4 and C_2H_2) systems. Further, in order to prove the possibility to deposit diamond without extra addition of H_2, measurements were also carried out for $Ar/CH_4/O_2$ and $Ar/C_2H_2/O_2$. With the usual mixtures of a few percent of hydrocarbon in hydrogen one can only take a look on the lower left side of the ternary C/H/O " diamond phase diagram", Fig. 1. With $Ar/CH_4/O_2$ and $Ar/C_2H_2/O_2$ mixtures it is possible to study regions which are usually only accessible with flame deposition methods. The other advantage of these mixtures is the decrease of the hydrogen content in the feed gas. By this way it is possible to control the influence of hydrogen on the deposition process.

Our results demonstrate that it is indeed possible to deposit diamond in a microwave reactor without extra hydrogen addition. However, in order to achieve diamond deposition it is necessary to reduce the $\bullet CH_3/H$ concentration ratio in the plasma by the addition of oxygen. Especially our mass spectroscopic data demonstrate that oxygen addition leads to the formation of H_2O and CO in the gas phase. With increasing oxygen concentration the production of C_2H_2 (from reactions of $\bullet CH_3$ radicals) for $Ar/CH_4/O_2$ decreases considerably. This is supported by the OES data which demonstrate that the intensity from C_1 species decreases more rapidly with oxygen addition than the H_α intensity We conclude, that in order to deposit diamond the $\bullet CH_3/H$ concentration ratio has to be below a well defined limit value; for higher methyl concentration the deposition of graphitic carbon (instead of diamond) occurs. Finally, our results suggest that oxygen can not only alter the plasma chemistry but can also substitute atomic hydrogen and efficiently etch (probably as OH) unwanted graphitic carbon deposition.

2. Experimental

The deposition experiments were carried out in a microwave plasma system (6), specially designed for the measuring of optical emission spectra. The process gases (purity better than 99.995%) were dosed with flow controllers (Ar: 100 sccm, else: 10 sccm) which had an accuracy of 0.5% F.S. A flow rate of 100 sccm argon and 7 sccm hydrocarbon was employed. The oxygen flow rate was varied between 0 and 7 sccm. During the two hours lasting deposition processes the pressure was kept at 15 torr. These deposition conditions were kept constant in all our experiments. After every deposition run an oxygen plasma was employed to clean the system from possible carbon residues.

The Si (111) substrates were heated separately. The temperature was controlled with a thermocouple placed in the molybdenum substrate holder and kept at 800 +/- 5 ^{0}C. The pretreatment of the substrates was performed by scratching with 0.25 μm diamond grit followed by an ultrasonic cleaning procedure.

The Raman spectroscopic measurements were performed with an Instruments S.A. U1000 double monochromator using the 488 nm line of an Ar ion laser.

The emission spectroscopy was made with an Spectroscopic Instruments system consisting of an Acton Pro 0.5 m monochromator equipped with a holographic 1200 lines/mm grating and an intensified 1024 diode array. The emission from the plasma was guided to the monochromator with an UV grade quartz fiber.

The mass spectroscopic measurements were carried out with an differentially pumped quadrupole mass analyzer (QMA) connected via a capillary to the deposition system.

3. Results and Discussion

3.1 Optical emission and mass spectroscopy

Fig. 2 shows two examples of optical emission spectra (OES) obtained from Ar/CH_4 microwave plasmas with different amounts of added oxygen. The emission band used in the present study to quantify gas phase species and radicals are labelled in Fig. 2 and compilated in table 1. We note, that the plasma intensities are not necessarily a direct measure of concentrations. The emission intensity can also be influenced by the electron energy distribution function of the plasma; further, for a high density plasma quenching and reabsorbtion of emitted light may play a considerable role. To overcome these problems actinometry can be used (5,7) by correlating intensities to an inert reference gas of known concentration. In our experiment we monitored the Ar line at 750 nm.

For the $Ar/CH_4/O_2$ system (Fig. 2) we observe that the H_α/Ar intensity ratio is nearly independent from the different oxygen content. However, we observe on the one hand a significant reduction of the C_2 signal and on the other hand an increase of the OH intensity. These results will be discussed below in more detail.

Generally we observed a linear correlation between the optical emission intensities and the plasma power input. Fig. 3 shows for example the linear increase of the H_α intensity for a H_2/CH_4 plasma (H_2 flow 100 sccm, CH_4) for increasing magnetron power input. The power input was determined from the product of electron emission current and magnetron high voltage. This result suggests that also a linear dependance holds under our experimental conditions for the emission intensity as function of plasma species concentration.

In the present study the OES measurements were complemented by mass spectroscopy (MS) using a differentially pumped quadrupole mass spectrometer to analyze the exhaust gases. Generally, these measurements do not allow the detection of metastable intermediates or radicals. Nevertheless, we can gain from the present data important informations about the plasma chemistry and its changes due to different gas feed compositions. As an example for the complemental informations of OES intensity measurements and exhaust gas concentrations we show in Fig. 4 the correlation between the C_2

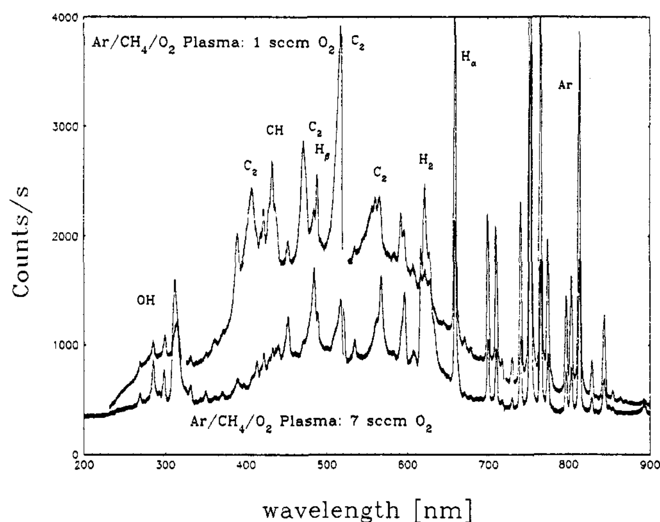

Fig. 2
Optical emission spectra obtained for $Ar/CH_4/_2$ plasmas

emission intensity and the acetylene (m/e = 26) mass spectrometer signal intensity for a $H_2/CH_4/O_2$ plasma. In this experiment H_2 and CH_4 was kept constant (100 sccm H_2; 7 sccm CH_4) whereas the oxygen addition was varied between 0 -7 sccm (oxygen atom fraction $X_{O:\Sigma}$: 0.0 - 0.35). As we will discuss below, due to the plasma reactions C_2 species are formed which are detected mainly as C_2H_2 in the exhaust by MS. Oxygen addition significantly decreases both the C_2 OES intensity and the production of C_2H_2. Within the confidence interval of 95% (Fig. 4) we find an acceptable linear correlation between both signal intensities. This result suggests that the C_2 OES intensity and the C_2H_2 production measured in

Table 1
Emission bands monitored for C/H/O plasmas during CVD diamond deposition (see also ref. (5)).

Species	Electronic Transition	Wavelength (nm)
Hα	2→3	656.3
OH	$A^2\Sigma+ \rightarrow X^2\Pi$	308.9
CH	$A^2\Delta \rightarrow X^2\Pi$(A-X)	431.2
C_2	$A^3\Pi_g \rightarrow X^3\Pi_u$	516.5
CO	$b^3\Sigma \rightarrow a^3\rightarrow\Pi$	283.3; 297.7
H_2	-	581.0
Ar	4p → 4s	750.4

duction measured in the exhaust are originating from the same plasma reaction.

3.2 Diamond depostion from $H_2/CH_4/O_2$ plasmas

Fig. 5 and 6 show OES and QMS measurements from H_2/CH_4 plasmas as function of increasing CH_4 concentrations. The quality of the deposited diamond layers were determined using Raman spectroscopy. For CH_4 concentrations below 2% the diamond deposition is manifested by an intensive

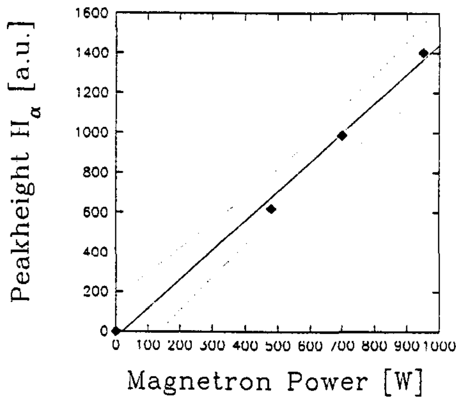

Fig. 3
H_α signal intensity from H_2/CH_4 plasma as a function of magnetron power input.

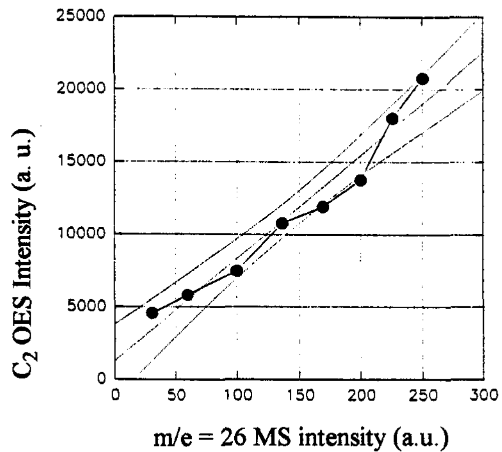

Fig. 4
Correlation between the C_2 OES and QMS C_2H_2 intensity signals for $H_2/CH_4/O_2$ plasmas. Due to the different amounts of oxygen addition, both OES (C_2) and QMS (C_2H_2) signals continuously decreases with increasing O_2 content.

peak located at 1332 cm^{-1}, which is identical to the Raman shift of natural diamond. For CH_4 concentrations above 1% the background signal from graphitic or amorphous carbon deposition continuously increases whereas the diamond peak at 1332cm^{-1} decreases and vanishes for > 2% methane.

The OES intensity measurements in Fig. 5 demonstrate that the H_α signal first increases between 0.0 and 0.5% CH_4 and above 0.5 % slightly decreases with increasing methane addition. Contrary, both the CH and C_2 signals continuosly increase with increasing CH_4 concentration. We note, that above 0.5% CH_4 the intensity ratio H_α/CH, which reflects the radical concentration ratio of •H/•CH_x, also increases continuosly. Our result suggests that this radical concentration ratio is an essential parameter for the diamond deposition. For an excess of •CH_x, the carbon deposition channel changes from diamond to graphitic or amorpheuos carbon.

Atomic H in the plasmas for diamond depositions is essential at least for two different reaction pathways. First, •H is needed for the production of •CH_x radicals, which are suggested to be the active species for diamond nucleation and growth. Further, atomic H is necessary for the removal of graphitic or amorpheuos carbon of the deposited films. We note that the carbon removal by atomic H is much faster for graphite than for diamond.

Fig. 6 shows the MS results for the same plasma experiment. Besides m/e = 16 (CH_4) and 26 (C_2H_2) we followed in this experiments also m/e =28 (C_2H_4, which can overlap with CO from the background pressure) and m/e = 18 (H_2O from impurities). We observe a continuos increase of both CH_4 and C_2H_2 signal intensities with increasing methane concentration. Above a concentration of 3% the C_2H_2 signal intensity exceeds that of CH_4. This behavior correlates quite well with the OES data of Fig. 5. To our opinion the C_2H_2 production reflects the increasing amount of •CH_x radical inside the plasma. Again, if the •CH_x concentration for constant atomic H exceeds a certain value, the deposition changes from diamond to graphitic or amorphous carbon.

In order to demonstrate the influence of oxygen addition for the diamond deposition process we show in Figs. 7 and 8 results of OES and MS experiments for a H_2/CH_4 plasma with a constant

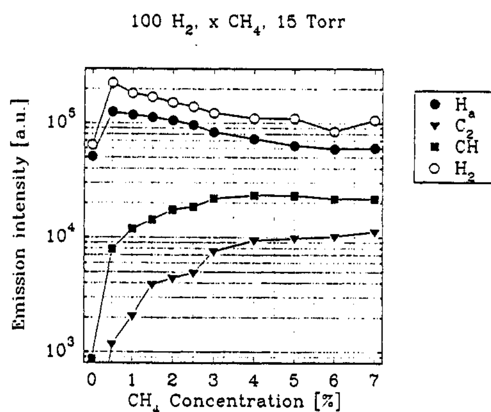

Fig. 5
OES signal intensities for an H_2/CH_4 plasma (15 Torr) a function of the CH_4 concentration. H_α (656.3 nm), C_2 (516.5 nm), CH (431.2 nm) H_2 (656.3 nm).

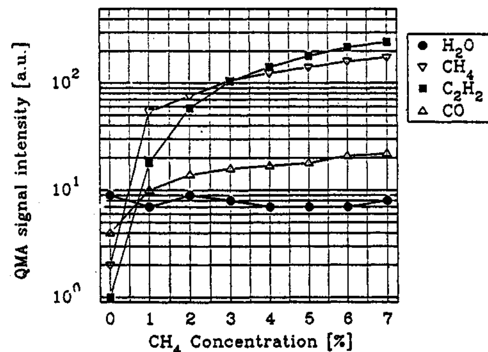

Fig. 6
QMS signal intensities for an H_2/CH_4 plasma (15 Torr) as a function of CH_4 concentration. CH_4 (m/e=16),C_2H_2 (26), H_2O (16) and C_2H_4 (m/e= 28).

methane concentration of 7%. Under this condition without any oxygen addition no diamond can be deposited; the high methane concentration leads to graphitic or amorphous carbon. However, Raman spectroscopy demonstrates that due to the addition of oxygen a "diamond window" opens for an oxygen atom fraction between $X_{O:\Sigma}$ from 0.03 - 0.05.

The OES measurements in Fig. 7 show that the oxygen addition has nearly no influence on the H_α intensity (constant atomic H concentration). However, the C and even more pronounced the C_2 intensity signals drop considerably with increasing oxygen concentration. This behavior again demonstrates that the •H/•CH_x concentration ratio determines the reaction channel to either diamond or graphitic (or amorphous carbon) deposition. When the •CH_x concentration ratio is too high (7% CH_4 without oxygen addition) only graphitic or amorphous carbon deposition occurs. Oxygen addition lowers the •CH_x concentration whereas the •H concentration nearly stays constant. The lack of any carbon deposition for $X_{O:\Sigma} > 0.05$ is believed to be due to the carbon removal by oxygen (probably through the reaction with OH).

The changes observed in the exhaust, Fig. 8, are in accordance with the interpretations derived from OES experiments. We observe only a slight decrease of the CH_4 signal with increasing oxygen content. However, the oxygen addition significantly decreases the C_2H_2 production. Again, this behavior reflects the decrease of •CH_x radical species within the plasma due to the oxygen. We note that no molecular O_2 can be detected while the plasma is burning. Molecular oxygen is instantly reacted and finally forms CO and H_2O.

3.3 Diamond deposition from $Ar/CH_4/O_2$ plasmas

Without the addition of oxygen it is not possible to deposit diamond from Ar/CH_4 or Ar/C_2H_2 feed gases (8), so the oxygen atom fraction $X_{O:\Sigma}$ = O/(O+H) is a critical parameter. In Fig. 9 the influence of oxygen addition on the film quality, as proved by Raman spectroscopy, is shown and in Fig. 10 the change of the exhaust gas composition, which reflects the change in the gas phase composition, is depicted. The reaction of the oxygen with the hydrocarbon in the plasma leads to the formation of water (m/e: 18) and carbon monoxide (m/e: 28). The acetylene (m/e: 26), which is produced by plasma reactions, is suppressed. The methane signal (m/e:16) stays nearly constant.

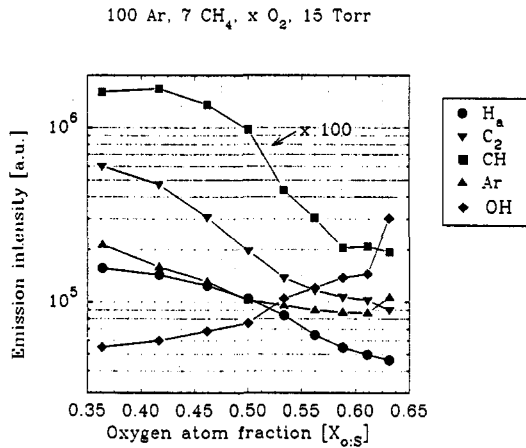

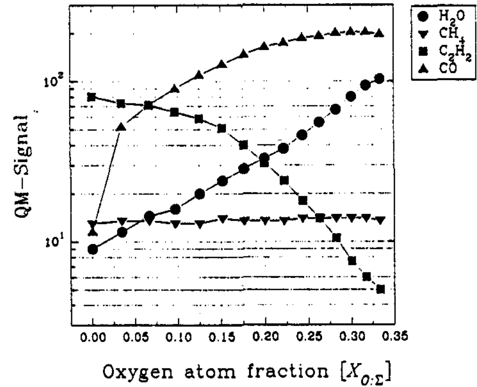

Fig. 7
OES signal intensities for an $H_2/CH_4/O_2$ plasma as a functon of the oxygen addition.
H_α (656.3 nm), C_2 516.5 nm), CH (431.2 nm) Ar (750.4 nm and OH (308.9 nm)

Fig. 8
QMS signal intensities for an $H_2/CH_4/O_2$ as a function of oxygen addition.
CH_4 (m/e=16),C_2H_2 (26), H_2O (16) and CO (m/e= 28).

The emission spectra prove the change in the gas phase composition. In Fig. 11 the variation of the intensity (peak area after background correction) of H_α (656.3 nm), C_2 (516.5 nm), CH (431.2 nm) and Ar (750.4 nm) is plotted against the oxygen content.

The decrease of the acetylene mass signal and the reduction of the C_2-signal in the emission spectra is accompanied by a drastic improvement of the phase purity. The deposition changes from graphitic to diamond almost instantaneously. The border for this change is located at an oxygen atom fraction $X_{O:\Sigma}$ of about 0.22. This corresponds to a change of the slope in the acetylene and the C_2-signal (Fig.10 resp.11), which could indicate a change in the kinetic reaction channels.

The decreasing growth rate is correlated with a decrease in the CH-signal intensity (5).

The intensity of the $H_\alpha$line shows a similar behavior as the Ar line, indicating an almost constant hydrogen dissociation in the plasma. Not shown in the figure is the growth of CO lines in the spectra. Emission lines of water molecules are not detectable in the spectra.

3.4 Diamond deposition from Ar/C2H2/O2 plasmas

In Fig. 12 the Raman spectra of diamond films deposited out of $Ar/C_2H_2/O_2$ feed gases with varying oxygen content are shown. Here the intrinsic hydrogen content from the hydrocarbon source gas is further reduced. The onset of diamond deposition is shifted to an oxygen fraction of about 0.5.

In Fig. 13 the variation of the emission spectra from $Ar/C_2H_2/O_2$ plasmas is shown. The CH-signal has been scaled by 100. In this figure the decrease of the C_2-signal is evident. For acetylene/oxygen mixtures the same conclusions as for methane/oxygen plasmas can be drawn. Diamond deposition takes only place if the acetylene content in the plasma is reduced.

In Fig. 14 the variation of the QMA signals of CH_4 (m/e: 16), H_2O (m/e: 18), C_2H_2 (m/e: 26) and CO (m/e: 28) in $Ar/C_2H_2/O_2$ plasmas are shown. If the oxygen fraction is increased beyond a

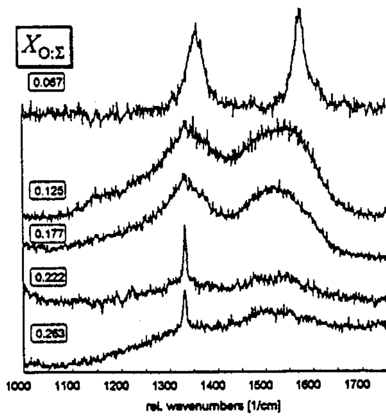

Fig. 9. Raman spectra of films deposited from $Ar/CH_4/O_2$ plasmas. From 0.067 (top) to = 0.263 (bottom) the oxygen atom fraction $X_{O:\Sigma}$ is increased.

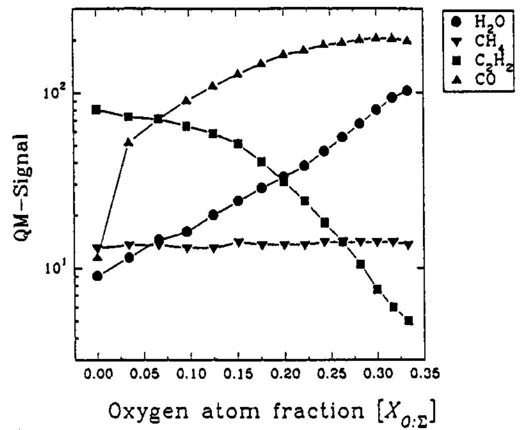

Fig. 10. Variation of the QMS signals of CH_4 (m/e=16), H_2O (18), C_2H_2 (26) and C (28) in $Ar/CH_4/O_2$ plasmas.

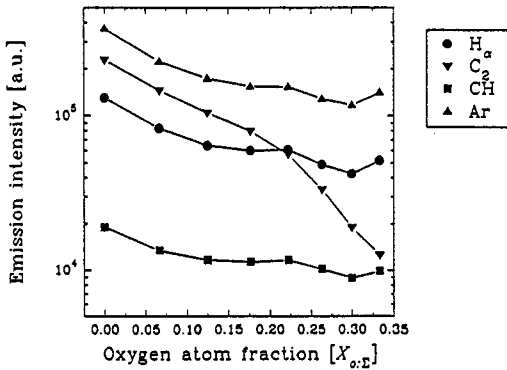

Fig. 11. OES signal intensities of H_α (656.3 nm) C_2 (516.5 nm), CH (431.2 nm) and Ar (750.4 nm) in $Ar/CH_4/O_2$ plasmas as a function of increasing oxygen concentration.

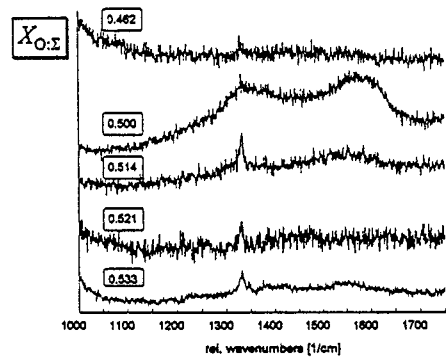

Fig. 12. Raman spectra of films deposited from $Ar/C_2H_2/O_2$ plasmas. The oxygen atom fraction $X_{O:\Sigma}$ is increased from 0.462 (top) to 0.533 (bottom)

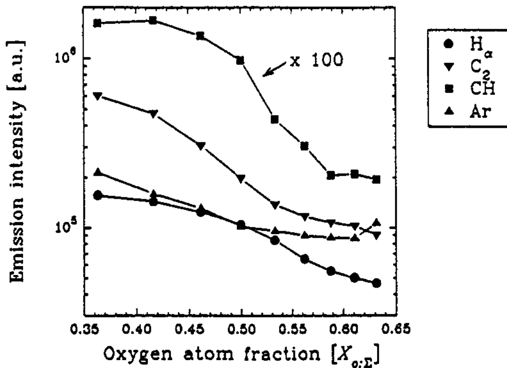

Fig. 13. OES signal intensities of H_α (656.3 nm) C_2 (516.5 nm), CH (431.2 nm) and Ar (750.4 nm) in $Ar/C_2H_2/O_2$ plasmas as a function of increasing oxygen concentration.

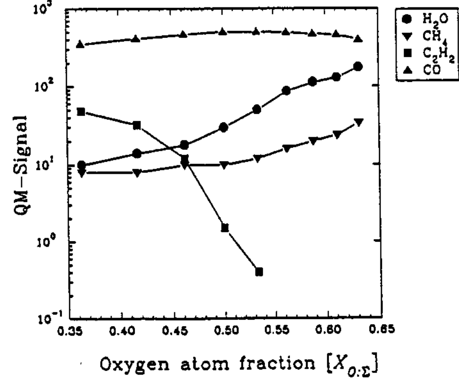

Fig. 14. QMS signal intensities of CH_4 (m/e=16), H_2O (18), C_2H_2 (26) and CO (28) in $Ar/C_2H_2/O_2$ plasmas as a function of increasing oxygen concentration.

value of about 0.55 the acetylene signal is no longer detectable. Spectroscopic measurements done by. Beckmann et al. (5) and own experiments show similar effects in conventional hydrogen/hydrocarbon feed gas mixtures. Our conclusion is that a substantial reduction in the acetylene content in the reaction plasma is necessary to deposit good quality diamond.

In comparison to the data supplied by Bachmann et al. (1) we find that the borders of our diamond deposition domain are shifted to the oxygen rich corner of the phase diagram.

4. Chemical reaction models

In Fig. 15 we propose a reaction scheme for $H_2/CH_4/O2$ and $H_2/C_2H_2/O_2$ gas mixtures in a microwave plasma. The reaction pathways which are assumed to be valid for this model are also summarized in Table 2. The temperature dependency of the rate constants k_i is assumed to be

$$k_i\,(cm^3/mol\bullet s) = k_{i0}\bullet T^{\nu}\bullet \exp(-E_a/RT)$$

The values for k_{i0}, ν and E_a are tabulated in Table 2. Without oxygen the reaction scheme is in accordance with a model proposed by Frenklach and Wang (9), which has recently be simplified by Lang and Störi (10). These authors demonstrated that the formation of hydrocarbons with more than two C atoms can be neglected. This assumption is in agreement with our MS measurements, which show the reaction of CH_4 to C_2H_2 (and partly to C_2H_4). C_3 and higher hydrocarbons, however, could not be detected. For a H_2/CH_4 plasma we assume that two main reaction channels are present for the formation of $\bullet CH_x$ radicals. The first is due to the dissociation of H_2 in the microwave plasma followed by a hydrogen abstraction reaction (reaction (3) in Table 2). The other channel, which is especially important for low H_2 concentration is the fragmentation of the hydrocarbons by electron impact from the plasma. According to Karoulina and Lebedev (11) the electron density function in a microwave discharge deviates from a maxwellian distribution. Higher electron energies which allow a ionization and fragmentation of molecules are available. As a first approximation we assume that similar fragmentation patterns of hydrocarbons occur inside the plasma as by electron impact inside a ionization chamber of a mass spectrometer. The typical fragmentations of CH_4 and C_2H_2 by electron impact are given in Table 3.

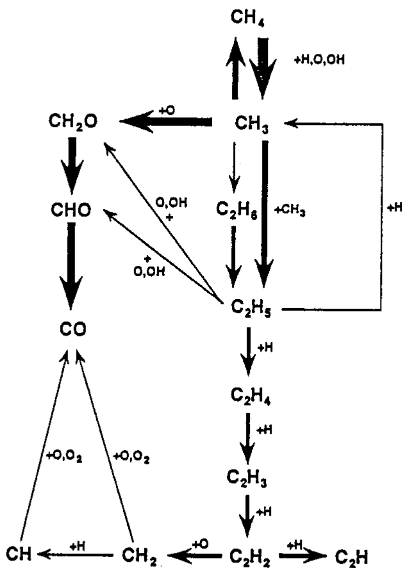

Fig. 15 Reaction scheme for $H_2/CH_4/O_2$ and $H_2/C_2H_2/O_2$ in a microwave plasma.

We note that the formation of $\bullet CH_x$ species by electron impact occurs for CH_4 with much higher probability as for C_2H_2. Therefore, the$\bullet CH_x$ production by electron impact should be small for C_2H_2. within the microwave plasma. However, for a H_2/C_2H_2. plasma, which was not studied in the present investigation, $\bullet CH_x$ formation is possible by a disproportioning reaction with atomic H (9).

The addition of oxygen reduces the $\bullet$ CH_x concentration in the microwave plasma. This result was demonstrated by OES and MS measurements. The reduction of $\bullet CH_x$ occurs via the reaction pathways(4), (5), (7) and (8).

Table 2
Reaction pathways occuring in a microwave plasma for $H_2/CH_4/O_2$ and $H_2/C_2H_2/O_2$ gas mixtures (see also ref. (10)).

Reaction	k_{i0}	ν	E_a ***(kJ/mol)***
1. $H + O_2 \rightarrow OH + O$	1.2×10^{17}	-0.91	69.1
2. $OH + H_2 \rightarrow H_2O$	1.0×10^{8}	1.6	13.8
3. $CH_4 + H \rightarrow CH_3 + H_2$	2.2×10^{4}	3.0	36.6
4. $CH_4 + O \rightarrow CH_3 + OH$	1.2×10^{7}	2.1	31.9
5. $CH_4 + OH \rightarrow CH_3 + H_2O$	1.6×10^{6}	2.1	10.3
6. $CH_3 + CH_3 \rightarrow C_2H_4 + H_2$	1.0×10^{16}	0	134
7. $CH_3 + O \rightarrow CH_2O + H$	7.0×10^{13}	0	0
8. $CHO + H \rightarrow CO + H_2$	2.0×10^{14}	0	0
9. $C_2H_5 + H \rightarrow C_2H_4 + H_2$	2.0×10^{13}	0	166
10. $CH_3 + CH_3 \rightarrow C_2H_5 + H$	8.0×10^{14}	0	11
11. $C_2H_4 + H \rightarrow C_2H_3 + H_2$	1.5×10^{14}	0	427
12. $C_2H_3 + H \rightarrow C_2H_2 + H_2$	2.0×10^{13}	0	0
13. $C_2H_2 + H \rightarrow C_2H + H_2$	6.0×10^{13}	0	99
14. $C_2H_2 + O \rightarrow CH_2 + CO$	4.1×10^{8}	1.5	7.1

Table 3
Fragmentation of CH_4 and C_2H_2 by electron impact in a mass spectrometer (12).

Gas	Fragmentation					
CH_4	CH_4 (44%)	CH_3 (37.1%)	CH_2 (7%)	CH (3.4%)	C (1.3%)	H (7.2%)
C_2H_2	C_2H_2 (72%)	C_2H (14.5%)	CH (4.5%)	C_2 (4.4%)	C_2H_3 (2.3%)	C (2.3%)

At the same time OH andO radicals form which are suitable species for the etching of unwanted graphitic or amorphous carbon deposition.

5. Conclusions

We briefly summarize the main conclusions of our present investigation.

1. Our OES and MS measurements demonstrate in good agreement with the "diamond phase" diagram by Bachmann et al. that the diamond deposition depends critically on the H/C/O ratio of the

feed gas. For a constant H/C/O ratio the diamond deposition using a microwave excitation is nearly independent from the source gas.

2. Diamond deposition is possible for $Ar/CH_4/O_2$ and $Ar/C_2H_2/O_2$ feed gases without extra addition of hydrogen. In this case OH and O radicals etch effectively unwanted graphitic or amorphous carbon deposition.

3. OES and MS measurements suggest that the "diamond window" requires a well-defined $\bullet CH_x/\bullet H$ concentration ratio inside the plasma. Outside this "diamond window" either graphitic or amorphous carbon (the $\bullet CH_x/\bullet H$ ratio is too high) or no deposition at all (the $\bullet CH_x/\bullet H$ ratio is too low) occur. The $\bullet CH_x/\bullet H$ ratio can be successfully adjusted by the addition of oxygen.

6. Acknowledgement

The investigations were supported by the Deutsche Forschungsgemeinschaft and the trinational German, Austrian and Swiss (D-A-CH) cooperational project "synthesis of super hard materials".

References

1. P. K. Bachmann, D. Leers, and H. Lydtin, Diamond and Related Materials, **1**, 1(1991)
2. O. Matsumoto, H. Toshima and Y. Kanzaki, Thin Solid Films 128 (1985) 341
3. Y. Saito, S. Matsuda and S. Nogita, J. Mater. Sci. Lett. 5 (1986) 565
4. W. Zhu, A. Inspekto, A. R. Badzian, T. McKenna and R. Messier, J. Appl. Phys. 68 (1990) 1589
5. R. Beckmann, R. Reincke, W. Kulisch, M. Kuhr and R. Kassing, Diamond and Rel. Mater., in press
6. P. Joeris, C. Benndorf, in *Surface Modification Technologies III,* ed. by T. S. Sudarshan and D. G. Bhat, The Minerals, Metals and Materials Society, Warrendale 1990, p. 61.
7. J. W. Coburn and M. Chen, J. Appl. Phys. 51 (1980) 3134
8. P. Joeris, C. Benndorf, and R. Kröger, Surf. Coatings Technol., in press
9. M. Frenklach and H. Wang, Phys. Rev. B 43 (1991) 1520
10. T. Lang, Dissertation, Technical University of Wien, 1992
11. E. V. Karoulina and Yu A. Lebedev, J. Phys. D: Appl. Phys. 21 (1988) 411
12. Index of Mass Spectral Data, American Society for testing Materails, 1969
13. J. Warnatz, in: Combustion Chemistry, Springer, New York, 1984